Getting a better understanding of the offshore marine boundary layer: Comparison between Large Eddy Simulation and offshore measurement data with focus on wind energy application

Beatriz Cañadillas[1], Thomas Neumann[2], Siegfried Raasch[3]

[1,2] DEWI GmbH - Deutsches Windenergie-Institut, Wilhelmshaven, Germany. E-mail[1]: b.canadillas@dewi.de
[3] IMUK - Institut für Meteorologie und Klimatologie, Universität Hannover, Germany

Abstract

In this work, Large-Eddy Simulations (LESs) have been performed and compared with observational data (FINO1 database), which will help us to gain a further understanding of offshore conditions. Shear-driven flows (under neutral and stable regimes) have been considered here because of their importance in wind energy applications. Not only mean values (profiles) are compared but also the turbulence unsteady effects are checked by using a statistical approach.

Notwithstanding the difficulty in interpreting the differences between both datasets ('idealized' simulation with observational data), they generally show good qualitative agreement in many areas with some differences that can be mostly explained by the sensitivity of the data to initial conditions, subgrid model parameterization and measurement uncertainties. In terms of gaining a physical understanding of the marine ABL, it is encouraging that the LES produces the same overall behavior as seen in the experimental observations.

1 Introduction

In the next years an increasing tendency towards offshore wind energy is expected world-wide [1]. Specifically in Germany, for instance, about 11,500 MW are planned to be installed by 2017 in the North Sea and Baltic Sea. One of the main reasons for 'going offshore' is the higher and more constant wind resource at sea than on land, resulting in significantly higher production per unit installed. At the same time, offshore wind farms are more costly to install and maintain than on land. Both installation and maintenance depend significantly on the marine conditions, i.e. the Marine Atmospheric Boundary Layer (MABL) which e.g. sets the limits for access and gives a basis for the layout of the wind turbine. Therefore, to make offshore wind farms economically feasible it is necessary to have a detailed knowledge of offshore conditions (MABL). Current knowledge of offshore conditions is very limited compared to conditions on land and this has placed growing importance on the necessity for research in this field.

2 LES Model Set-up

Here a Parallelized Large-Eddy Simulation Model (PALM) has been used. It solves the non-hydrostatic Boussinesq approximated Navier-Stokes equations and uses a 1.5-order subgrid

closure scheme. Monin-Obukhov similarity theory is assumed between the surface and the first computational grid point of the model domain. For details and features of the LES code, please refer to [2] and to the on-line PALM documentation (http://www.muk.uni-hannover.de/~raasch/PALM group/PALM group.html).

In this work, an idealized marine ABL simulation is performed over a flat and uniform surface where the Charnock parameterization [3] is used at the bottom-surface to characterize the sea roughness (z_0). The simulation is run for 123, 200 sec time period (≈32.2 hours), with a neutrally stratified boundary layer developed during the first 80, 000 sec with a potential temperature assumed constant over the entire domain (settled at θ_0 = 290.5 K, based on the mean value determined from the FINO1 data) and zero surface heat flux. Afterwards, during the next 43, 200 sec of the run, the surface heat flux is progressively reduced from 0 to −0.05 mKs^{-1} to generate a stable ABL with different grades of stratification. This forcing method for developing the SBL has been previously used by several authors (e. g. [6],[7],[8]).

To deal with the limited domain size of the model, cyclic boundary conditions are applied in both horizontal directions. The Coriolis parameter is set to $f_c = 1.181 \cdot 10^{-4}\ s^{-1}$, corresponding to a latitude of about 54°N (where the FINO1 platform is located). The grid spacing is isotropic along all directions except vertical, where in order to limit the number of grid points and so save computational time; a stretching factor (8%) is applied above 600 m up to the top of the model where the maximum resolution allowed is 10m. The last hour of each section is used to compute the statistics for analysis.

A summary of the simulation setup (chosen according to several sensibility tests carried out) is presented in Table 1, where L_x, L_y, L_z are the widths of the computational domain, N_x , N_y , N_z are the number of grid points and Δx , Δy , Δz define the grid size in the x-, y- and z-directions, respectively.

(ug,vg)	***LxxLyxLz [m3]***	***NxxNyxNz***	***ΔxxΔyxΔz [m3]***
(14, 0)	2560x1280x1371	512x256x152	5x5x5

Table 1: Summary of the LES simulations.

2.1 Bulk Parameters

Table 2 provides a summary of the resulting bulk parameters typically examined in BL studies and computed during the last hour of each section as the heat fluxes decrease. Parameters included in this summary are: turbulent BL height (δ), stability parameter (zL^{-1}), friction velocity (u_*), averaged time step (dt) and strength of surface cooling ($\Delta\theta_s$).

ID	$w\theta_s$	***δ[m]***	zL^{-1} ***[-]***	$u_*[m^{s-1}]$	***dt [sec.]***	$\Delta\theta_s$ ***[K]***
N	0.0	1140	0.00	0.37	0.29	-
S1	-0.005	1095	0.02	0.33	0.29	0.2
S2	-0.01	375	0.04	0.31	0.28	0.7
S3	-0.02	225	0.10	0.28	0.27	1.9
S4	-0.03	150	0.19	0.26	0.26	4.1
S5	-0.04	145	0.28	0.25	0.26	7.1
S6	-0.05	135	0.40	0.24	0.25	11.2

Table 2: Bulk parameters of the simulated ABL evolution for $u_g = 14ms^{-1}$.

The turbulent boundary layer height (δ) is computed as (1/0.95) times the height at which the horizontal shear stress has dropped to 5% of its surface value [10]. It can be seen that, as stability increases, the turbulent BL height decreases.

According to [11] , weakly ($0.00< zL^{-1}<0.06$) and moderately ($0.06< zL^{-1}<1$) stable regimes are simulated here. Friction velocity decreases as stability increases. Regarding the time step, it decreases as the stability increases as expected.

2.2 Mean and Turbulent Vertical Structure

Fig. 1 shows the vertical profiles of horizontal wind speed, wind angle, turbulence intensity (TI), the ratio between the SGS scale and the total (resolved+subgrid) turbulent kinetic energy (TKE), potential temperature and non-dimensional horizontal kinematic shear stress for u_g=14ms^{-1} geostrophic wind prescribed when the surface heat flux decreases (starting from the neutral regime). Profiles presented are both time-averaged and averaged over horizontal directions.

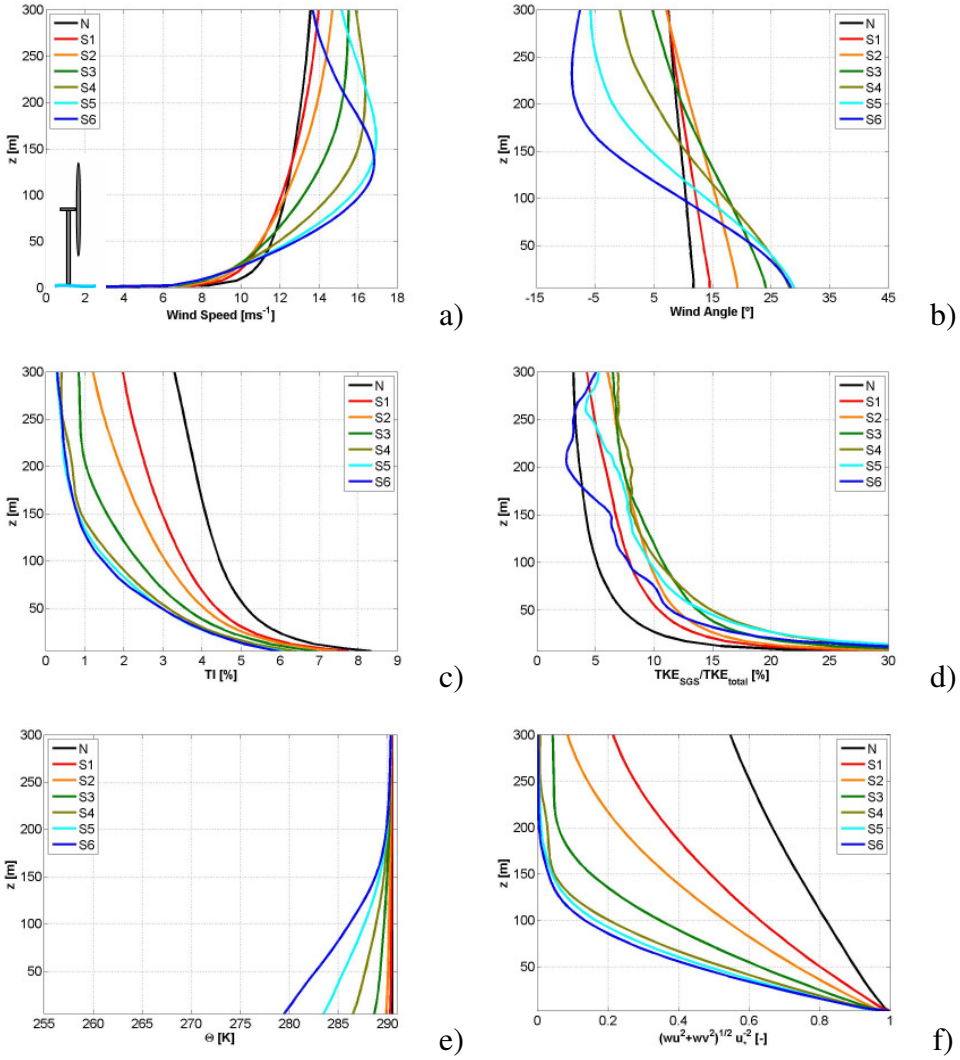

Figure 1: Evolution of the mean profiles as surface cooling increases: wind speed (a), wind angle (b), turbulence intensity (TI) (c), ratio between the SGS scale and the total TKE (d), potential temperature (e), non-dimensional shear stress (f) for u_g = 14 ms^{-1}. Acronyms shown in the legend correspond to N for neutral regime and from S1 to S6 for $\langle w'\theta' \rangle$ = -0.005, -0.01, -0.02, -0.03, -0.04 and -0.05 mKs^{-1} respectively. Note that only the first 300 m above the surface are plotted.

From the evolution of the mean wind speed profile, there can be seen a clear increase of the shear (increase of wind speed with altitude) as the stability increases, which displays development of a low level jet (LLJ) near the top of the boundary layer in the last stage of stable profiles. Boundary layer heights range from 1140m (neutral) to about 135m (most stable cases). The angle between the surface wind direction and the geostrophic wind simulated increases with stability. Values obtained range from about 11º in the neutral regime to about 30º in the stable regime.

As expected, TI is strongest near the ground, decreasing from a high to zero. An evident reduction of TI as stability increases is apparent.

The non-dimensional horizontal shear stress decreases almost linearly with height from a maximum value of about 1.0 on the surface to zero at the top of the boundary layer for all stabilities. This is an indication that the flow has reached a quasi-steady state. Moreover, as the boundary layer gets more stable, the shear stress decreases.

The potential temperature profiles clearly show a two-layer structure in the stable profiles: a stable surface layer with strong gradients and a constant θ layer (zero gradient). The strength of inversion increases with the (negative) surface heat flux which thereby leads to an increased suppression of turbulent mixing and hence a decay in the turbulent layer height.

It is well known that the size of the dominant turbulent eddies decreases as the atmospheric stability increases and therefore small grid resolutions are necessary in order to resolve most of the turbulent motion of the flow. Otherwise the contribution of the SGS model comes into play and the results can be quite sensitive to the type of parameterization used to represent the subgrid (SGS) scales (smaller than the grid size). Near the surface, it is expected that as the stability increases from neutral to stable, the ratio between the SGS scale and the total TKE (Fig. 1, right side of the bottom-panel) should increase. It can be clearly seen that for the most stable cases simulated, the opposite is found (see profiles S4, S5, S6). This unphysical behaviour of the profiles has been found by other authors (e.g. [5], [6]) and has been attributed to a failure of the SGS model. That problem is a well-known limitation in modeling where such a flow conditions are very difficult to simulate due to the intermittent nature of the turbulence. Therefore, in order to simulate the most stable cases a higher resolution should be used, however at FINO1 location such stable conditions were not found for the period used in this work (see Fig. 2).

3 LES versus FINO1. Profile comparison

In this section, the simulations performed in section 2 are tested along vertical profiles by selecting three parameters of considerable practical interest from a wind energy perspective (wind shear, wind direction and TI). For this purpose a two year (2005-2006) database from the offshore mast FINO1 station [3] located 45 km off Borkum Island (lat. 54°0.870N, long. 6°35.240E) in the North Sea is used. The comparison is limited to the three sonic anemometers available at the FINO1 location and placed at heights of 40, 60 and 80 m.

We are aware that since the simulations carried out in this work are idealized cases, a quantitative agreement between the simulation results and the observations is not expected but this will give us a guide to the relative performance and sensitivity of the model.

3.1 Data Selection for Comparison Purposes

In order to perform the comparison between observations (FINO1) and the idealized LES simulations, FINO1 database is classified as follows:

- First, FINO1 surface heat flux data (<w'θ'>) are categorized into different ranges according to the surface heat flux forcing applied in LES simulations.

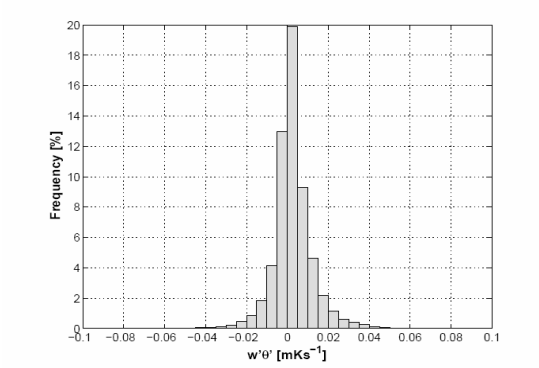

Figure 2: Probability distribution function of sensible heat flux <w'θ'> for the studied period at FINOl location.

- Second, the observed wind at 30 m is used (since no estimates of geostrophic winds are available from FINO1 data) to perform a sub-classification for each range of observed surface heat flux according to the simulated wind at 27.5 m (the closest height to 30m).

Moreover, rain-periods and humidity above 70% are excluded. This methodology is similar to the one used by [9].

Fig. 3 shows the profile comparison for neutral and weakly stable regimes. FINO1 data are depicted as bin-median values with bars representing one standard deviation of the data in each data range.

Atmospheric measurements reveal a rather large scatter. This can be explained mainly by the complex interplay of different forces in the real atmosphere. Nevertheless, the qualitative agreement between both sets of data is rather good with most of the simulation results falling within the error bars of the FINO1 data. Moreover, the calculation of the surface heat fluxes from the FINO1 data used for the data classification is in some way not free of uncertainties and this can generate some discrepancies in the classification as well as the way of data classification itself. On the other hand, LES simulations have also several uncertainties and their results are sensitive to grid resolution and initial conditions, amongst others, especially under stable conditions. Therefore, LES simulations should be considered also with bars.

Neutral regime:

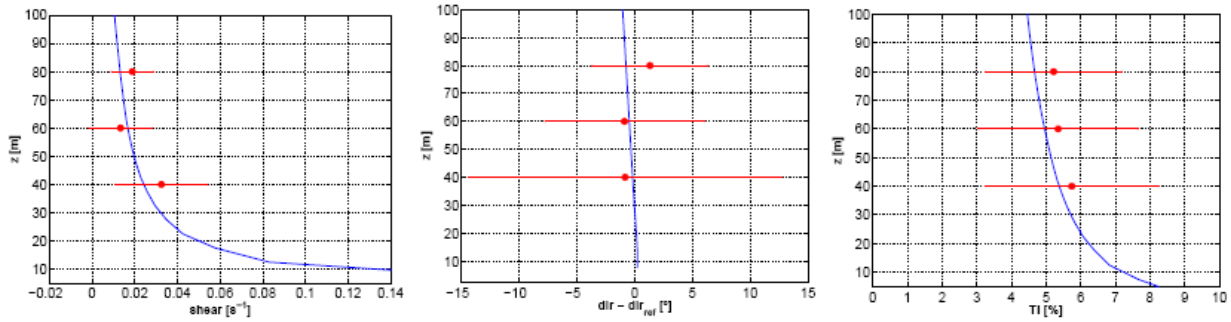

Weakly stable regime (<w'θ'> = - 0.01 mKs^{-1}):

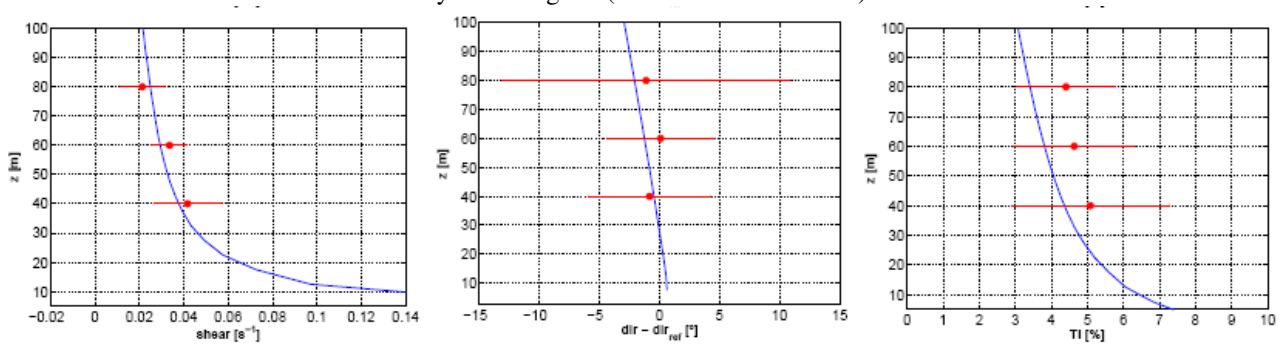

Figure 3: Comparison of profiles between simulated (blue) and measured (red) data. Vertical wind shear (left side of the panel), horizontal wind direction (middle side of the panel) and TI (right side of the panel). ***u_g = 14 ms^{-1}***

4 Further Analysis: Time Series

The profile comparison performed in section 3 provided a measure of the mean characteristics of turbulent flow, although when information about unsteadiness (eddy structures) is desired, a statistical approach is required and therefore a time series is needed.

For this purpose, one point at the centre of the LES domain has been selected to generate time series at 80 m of the horizontal wind velocity components (longitudinal (u), transverse (v)) to compare with one- point FINO1 measurements. A neutral simulation with u_g = 10 ms^{-1} and 2m grid resolution was performed. Model set-up was as described in section 2.

4.1 Comparison between 2 m resolution LES-simulation and FINO1 data

The power spectrum density obtained from the FINO1 data and LES simulation (2m resolution) is shown in Fig. 4 under neutral regime. The black line shows the theoretical slope of the Kolmogorov inertial sub-range ($f^{-2/3}$). The vertical gray line is a roughly estimated cut-off frequency (f_{cutoff}) for the LES simulation which corresponds to the frequency at which the results of LES begin to decline in comparison with measurements. Practically, the simulation cannot predict frequencies higher than f_{cutoff}.

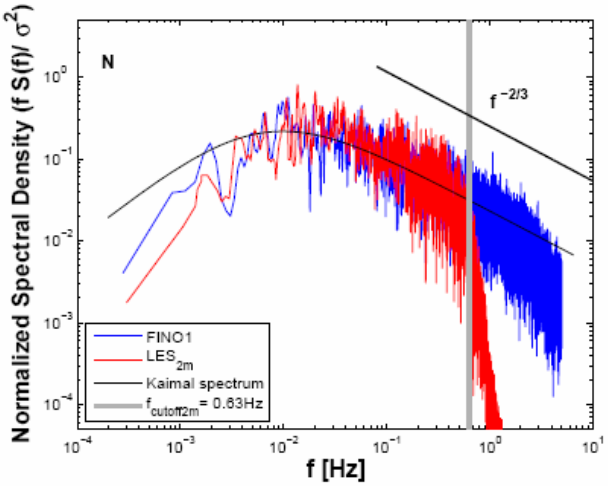

Figure 4: Normalized one-dimensional spectra of the horizontal wind velocity fluctuations: LES simulations (red) and FINO1 data (blue). Black curve represents the Kaimal model spectrum.

As it can be seen in Fig. 4, due to the limited resolution of the grid and due to the SGS model, the turbulent spectra from the LES simulation does not show the extended inertial range found in the measured data. However, at low frequencies, the spectral shape of the simulation follows measurements reasonably well.

Moreover, the statistics of velocity increments ($U_\tau(t) := U(t + \tau) - U(t)$ where $U_\tau(t)$ denotes the wind speed at time t and scale τ) are also investigated in order to characterize the flow gust behavior [13]. In Fig. 5 the probability density functions (PDFs) of the normalized U_τ for different τ values are shown. It should be mentioned that both data were filtered by using a top-hat filter at the cut-off frequency (f_{cutoff}).

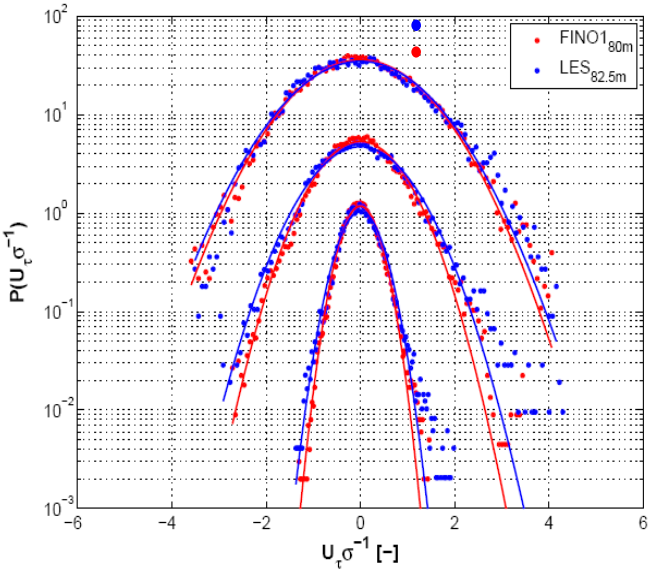

Figure 5: PDFs of velocity fluctuation increments at τ = 1, 3, 10 sec respectively (bottom-up). Red (blue) filled circles denote simulated (measured) data. The standard Gaussian distribution is indicated by solid lines. PDFs are shifted vertically by an offset of 10.

It is evident from Fig. 5 that, LES simulation is able to reproduce fairly the 'intermittence' of the flow. However, FINO1 PDFs show more open tails than LES values suggesting higher extreme values present in FINO1 data. This discrepancy may be partly attributed to the grid resolution.

5 Conclusion

In this work LES model performance has been presented and tested with observational data through vertical profiles as well as statistical approach in order to get a more complete picture of the flow.

Notwithstanding the difficulty in interpreting the different nature of both datasets ('idealized' simulation with observational data), they generally show good qualitative agreement with some differences that can be mostly explained by the sensitivity of the data to initial conditions, subgrid parameterization (SGS model), data classification procedure and measurement uncertainties. In terms of gaining a physical understanding of the marine ABL, it is encouraging that the LES produces the same overall behavior as seen in the experimental observations.

6 Acknowledgements

This has been supported by ModObs, Marie-Curie Early Stage researcher program (MRTN-CT-2005-019369), financed by European Commission.

7 References

[1] DEWI GmbH Deutsches Windenergie-Institut. Wind energy study 2008. Assessment of the wind energy market until 2017. Technical report, *DEWI Magazin*, 2008.

[2] S. Raasch and M. Schröter. PALM: A large-eddy simulation model performing on massively parallel computers. *Meteorologische Zeitschrift*, 10:363–372, 2001.

[3] T. Neumann, K. Nolopp, and K. Herklotz. First operating experience with the fino1 research platform in the North Sea. *DEWI Magazin*, 24, 2004.

[4] H. Charnock. Wind stress over a water surface. *Quarterly Journal of the Royal Meteorological Society*, 81:639–640, 1955.

[5] P. J. Mason and S. H. Derbyshire. Large-eddy simulation of the stably-stratified atmospheric boundary layer. *Boundary-Layer Meteorology*, 53:117–162, 1990.

[6] E. M. Saiki, Chin-Hoh Moeng, and Peter P. Sullivan. Large-eddy simulation of the stably stratified planetary boundary layer. *Boundary-Layer Meteorology*, 95:1–30, 2000.

[7] F. Ding, S. P. Arya, and Yuh lang Lin. Large-eddy simulations of the atmospheric boundary layer using a new subgrid-scale model ii. weakly and moderately stable cases. *Environmental Fluid Mechanics*, 1:49–69, 2001.

[8] M. A. Jiménez and J. Cuxart. Large-eddy simulations of the stable boundary layer using the standard Kolmogorov theory: Range of applicability. *Boundary-Layer Meteorology*, 115:241–261, 2005.

[9] M. A. Jiménez. Stability stratified atmospheric boundary layer: Study through Large Eddy Simulation, mesoscale modeling and observations. PhD thesis, Universitat de les Illes Balears, September 2005.

[10] B. Kosovíc and J. Curry. A large eddy simulation study of a quasi-steady stably stratified atmospheric boundary layer. Journal of Atmospheric Sciences, 57:1052–1068, 2000.

[11] L. Mahrt. Nocturnal boundary-layer regimes. *Boundary-Layer Meteorology*, 88(2):255–278, 1998.

[12] IEC61400-1. Wind turbines-part 1: Design requirements. Technical report, International Electrotechnical Commission (IEC), 2005.

[13] J. Peinke, S. Barth, F. Böttcher, D. Heinemann, and B. Lange. Turbulence, a challenging problem for wind energy. *Physica A: Statistical Mechanics and its Applications* 338:187–193, 2004.